This is an Accepted Manuscript version of the following article, accepted for publication in:

A. Arruti, A. Agote, I. Aizpuru and M. Mazuela, "Exploration of Steinmetz Parameter Variability in High Frequency Transformer Design Spaces," *2025 Energy Conversion Congress & Expo Europe (ECCE Europe)*, Birmingham, United Kingdom, 2025, pp. 1-6.

DOI: https://doi.org/10.1109/ECCE-Europe62795.2025.11238738

Exploration of Steinmetz Parameter Variability in High Frequency Transformer Design Spaces

Asier Arruti
Electronics and Computing Department
Mondragon Unibertsitatea
Hernani, Spain
aarruti@mondragon.edu

Anartz Agote
Electronics and Computing Department
Mondragon Unibertsitatea
Hernani, Spain
aagote@mondragon.edu

Iosu Aizpuru
Electronics and Computing Department
Mondragon Unibertsitatea
Hernani, Spain
iaizpuru@mondragon.edu

Mikel Mazuela
Electronics and Computing Department
Mondragon Unibertsitatea
Hernani, Spain
mmazuela@mondragon.edu

Abstract- This paper investigates the impact of high frequency effects in the design space of transformers for power converters. A holistic overview of the impact of winding losses has previously been studied in the literature, but such an analysis is missing for the high frequency effect of the core. This work will address this issue by using variable Steinmetz parameters to model the non-linear behavior of core losses at high frequencies, while retaining a holistic view of the transformer design. Classical transformer scaling laws and high-frequency winding loss models are reviewed and combined with the improved non-linear core loss model. To demonstrate the improved model the optimal (minimum losses) solution for a case study is identified and compared against solutions from simplified core loss models.

Index Terms- High-frequency transformers, Power transformers, Transformer design, Core losses.

I. Introduction

CLASSICALY, the volume occupied by a power transformer is linked directly to the working frequency. As switch technology is improved, the transformer can be further optimized, which allows for improvement in the volume and losses of the device. Unfortunately, it is known that these improvements due to increased frequency are limited at high frequencies due to increased losses and decreased cooling capacity [1].

With the adoption of high-performance Wide Band Gap (WGB) switches, the barriers for power converter efficiency and power density are pushed forward [2], [3], but optimal solutions require a great understanding of the limitations of the transformer design at high and very high frequencies.

The analysis of these limitations has commonly focused on the windings, which are critical due to eddy losses in the copper at high frequencies. Nevertheless, planar magnetic cores and transformers are becoming more and more relevant in addressing the increase in copper losses, allowing to push higher frequencies [4]-[7].

The other relevant problem at high frequencies is the rapid increase in core losses. Not only does a higher fundamental frequency increase the losses, but more complex modulation strategies and flux density waveforms can also increase the losses by factors of 100 % [8]. Recently this research topic has gained noticeable focus, with [9] being a clear indicator of this.

Still, these works limit the focus on improving modelling techniques for core losses by means of experimental data. Holistic analyses of the classical transformer design space and considerations of the high frequency effects in the windings exist, but not for core effects. Even though many assumptions are made to approach the problem in a generic way, the obtained results and tendencies still serve to better understand design scaling laws and limitations.

The focus of this work is to present a holistic analysis based on well-known transformer basic design rules in combination with the previously published high frequency winding effects. To do so, this paper is structured in the following chapters:

1. First, the paper will focus on giving an overview of the classical transformer design rules and scaling laws, resulting in a transformer design space.
2. Second, the impact of the high frequency effects in the windings will be added to the design space.
3. Lastly, the variability of the Steinmetz parameters will be implemented in the design space, showing how these can negatively impact the design space.

To validate the results, a case study is presented, and the optimal (minimum loss) solutions from existing techniques and considering the variability of core losses from this work are identified and compared.

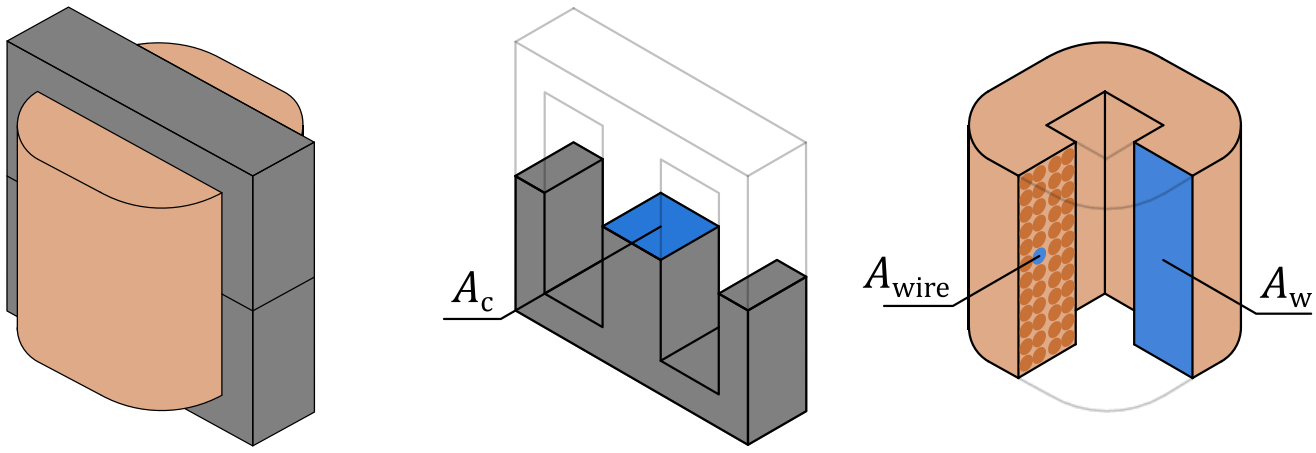

a) b) c)

Fig. 1: a) General transformer geometry with EE core configuration considered in this study. b) View of the transformer and its magnetic cross section or area A_c and c) view of the winding and the winding area A_w and wire area A_{wire}.

II. Basis of Transformer Design Space

To understand the complexity on the design space of high frequency magnetics, first the basis of classical transformer design scaling laws must be understood. The generic transformer geometry studied in this work is shown in Fig. 1.

The design space of a classical transformer can be derived by pre-selecting certain specific design parameters. Electrically, two parameters are critical, the voltage applied to the transformer and the current in the windings. If the voltage V is known, the flux density B in the magnetic core can be expressed as

$$B = \frac{\sqrt{2}V_{\mathrm{RMS}}}{2\pi f N A_c} \tag{1}$$

with f being the frequency, N being the number of turns and A_c being the magnetic cross section of the core. Similarly, by setting a design current density J (commonly between 3 and 6 A/mm^2) the relation

$$J_{RMS} = \frac{2I_{RMS}N}{K_w A_w} \tag{2}$$

with K_w representing the fill factor (commonly between 0.5 and 0.7) and A_w is the core winding area.

Combining (1) and (2) results in

$$\mathcal{P} = V_{RMS} I_{RMS} = A_w A_c \frac{1}{\sqrt{2}} J_{RMS}\, K_w B \pi f \tag{3}$$

which relates the main transformer key design parameters with the apparent power applied to the transformer. Note that the geometrical definitions of the core A_w and A_c appear grouped together, thus by defining the area product $A_p = A_w A_c$ the core can be chosen based on the application apparent power $\mathcal{P}$.

With (3) defined (classically called the power equation), the next step in the classical design is to estimate the copper and core losses. For the copper losses the expression

$$P_w = \frac{v_w}{\sigma}\left(\frac{2I_{RMS}}{K_w A_w}\right)^2 N^2 \tag{4}$$

can be used, where v_w is the volume occupied by the windings and σ the conductivity. Similarly, using the Steinmetz parameters k, α and β [10], the expression

$$P_c = v_c k \left(\frac{\sqrt{2}V_{RMS}}{2\pi A_c}\right)^{\beta} f^{\alpha-\beta} N^{-\beta} \tag{5}$$

is obtained, where v_c is the volume of the core.

By combining (4) and (5), the total losses P_t are then

$$P_t = \frac{v_w}{\sigma}\left(\frac{2I_{RMS}}{K_w A_w}\right)^2 + v_c k \left(\frac{\sqrt{2}V_{RMS}}{2\pi A_c}\right)^{\beta} f^{\alpha-\beta} N^{-\beta}. \tag{6}$$

The minimum loss design (optimal solution considered for this analysis) is that which leads to the minimum value for P_t. The distribution of losses between winding and core can be adjusted with the number of turns N, thus $\partial P_t / \partial N = 0$ will lead to

$$N_{opt} = \left(\frac{BC_c f^{\alpha-\beta}}{2C_w}\right)^{\frac{1}{\beta+2}} \tag{7}$$

with the coefficients

$$C_w = \frac{v_w}{\sigma}\left(\frac{2I_{RMS}}{K_w A_w}\right)^2 \tag{8}$$

$$C_c = v_c k \left(\frac{\sqrt{2}V_{RMS}}{2\pi A_c}\right)^{\beta} \tag{9}$$

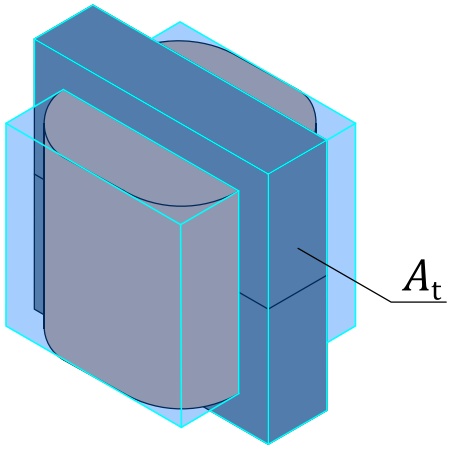

Fig. 2: Cooling area used for the single thermal resistance model used in this study.

resulting in the optimal N_{opt} to minimize the losses. Since C_w increases to the power of 2 while C_c increases to the power of β, the optimal design points is found at $P_c/P_w = 2/\beta$.

The last step in the design process is to estimate the temperature of the selected transformer due to the power losses. Higher complexity thermal models exist in literature, but with the aim to obtain a holistic view of the design space, the single thermal resistance approximation from [11] is used in this work. According to this approximation, for a known cooling are A_t the temperature rise of the transformer is

$$\Delta T = \left(\frac{P_t}{10 \cdot A_t}\right)^{\frac{1}{1.1}}. \tag{10}$$

The cooling area used in this work is that shown in Fig. 2.

Taking these classical transformer design rules and scaling laws, an overview of the transformer design space can be obtained. To do so, first the properties of the transformer must be defined, including the application voltage and currents, as well as the maximum allowed temperature rise, and the specification of the core and windings. The parameters used in this study are shown in TABLE I. For the Steinmetz parameters, the low frequency set (f < 300 kHz) from [10] is used.

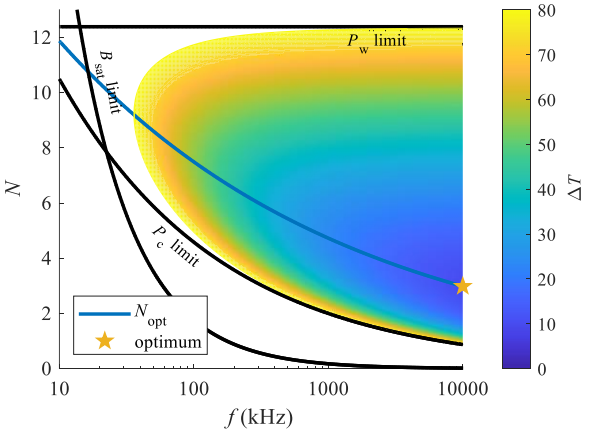

Fig. 3: Transformer design space obtained by using the classical low frequency transformer design rules.

TABLE I: Design Specifications (equations are defined for SI units)

Application	V_{RMS}	300 V
	I_{RMS}	10 A
	ΔT	80 ºC
Core	Type	EE80/30/20
	A_c	400 mm^2
	A_t	25600 mm^2
	v_c	80000 mm^3
	Material	3F3
	k	0.5 (f < 300 kHz) $2 \cdot 10^{-2}$ (300 < f < 500 kHz) $36 \cdot 10^{-7}$ (f > 500 kHz)
	α	1.6 (f < 300 kHz) 1.8 (300 < f < 500 kHz) 2.4 (f > 500 kHz)
	β	2.5 (f < 300 kHz) 2.5 (300 < f < 500 kHz) 2.25 (f > 500 kHz)
	B_{sat}	300 mT
Winding	K_w	0.6
	σ	58 MS/m
	A_w	1200 mm^2
	v_w	192000 mm^3
	ς_w	$1 \cdot 10^{-12}$

The design space obtained is shown in Fig. 3. The saturation flux density limit has been added, although it is not limiting for the selected analysis. Here, one can see how as the frequency increases, since the volt-seconds applied to the transformer decrease, the flux density has the natural tendency to decrease, and as long as $\alpha < \beta$ this means that the core losses are reduced. Because of this, the number of turns can be decreased to obtain a solution with lower overall losses and temperatures. The optimal case is at the maximum available frequency. The point with the minimum losses at a given frequency is that obtained from (7).

III. High Frequency Winding Effects in the Design Space

In reality, there are several practical limitations due to high frequency effects limiting the available design space, which can be divided into high frequency effects in the windings and the core.

The increase in winding losses at high frequencies and eddy currents is a well-documented and investigated topic. Unfortunately, this is a closely dependent on the wire geometry (solid, litz, foil) and even the winding geometry. To consider this effect into the design space, a more holistic approach is required to model this effect, thus the methodology proposed in [12]-[15] is used for this paper.

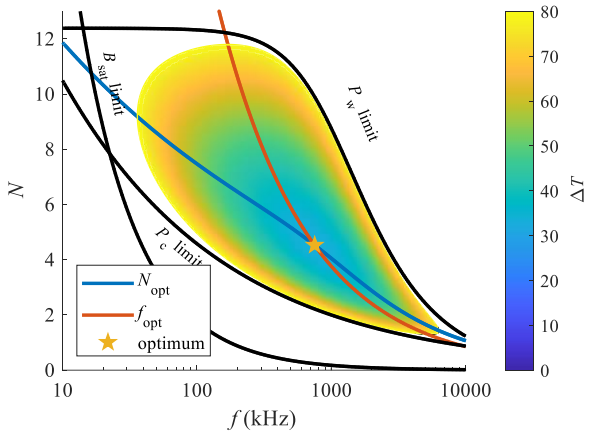

Fig. 4: Transformer design space taking the high frequency effects in the windings into consideration.

The most general way to consider the increase in winding losses is to modify (4) as

$$P_w = (1 + \varsigma_w f^2) C_w N^2 \tag{11}$$

and use the ς_w parameter. With the aim of obtaining a holistic view of the design space, $\varsigma_w = 1 \cdot 10^{-12}$ is selected, meaning that the winding losses increase by 100 % at 1 MHz. This value is lower than what is expect for a 3 kVA transformer, but it allows to obtain a better view of a wide design space and better analyze and examinate the impact of other effects in the design space.

With the modification (11), now the optimal solution also changes, by rewriting (6), now two optimal solutions can be found by solving $\partial P_t / \partial N = 0$ and $\partial P_t / \partial f = 0$. In this case two expressions are obtained for the optimal solutions,

$$N_{opt} = \left(\frac{B C_c f^{\alpha-\beta}}{2 C_w (1+\varsigma f^2)} \right)^{\frac{1}{\beta+2}} \tag{12}$$

for the optimal number of turns at a given frequency and

$$f_{opt} = \left(\frac{2}{\beta-\alpha} \frac{C_w \varsigma_w}{C_c} N^{\beta+2} \right)^{\frac{1}{\alpha-\beta-2}} \tag{13}$$

for the optimal frequency at a given number of turns. The true optimal solution is the solution which fulfills both (12) and (13).

With these modifications in mind, the new design space is shown in Fig. 4. Notice now how the design space is limited at high frequencies due to the increased winding losses. Still, with the selected low ς_w value the optimal solution appears at 747 kHz, precisely where the N_{opt} and f_{opt} line intersect. Recalling back to the parameters from TABLE I, an alternative set of core loss Steinmetz parameters is given for frequencies higher than 500 kHz [10], where the optimal solution is found at.

IV. High Frequency Core Effects in the Design Space

It is clear by comparing the design space from Fig. 4 and the Steinmetz parameters from TABLE I that the optimal solution from Fig. 4 is inaccurate. To estimate the accurate optimal solution, the design space analysis should be realized with the appropriate Steinmetz parameters for each frequency. Thus, working at f < 300 kHz the first set of parameters should be chosen, but at f > 300 kHz the second or third set of parameters should be used.

Since the β value of both the first and second set of Steinmetz parameters is the same, the only boundary in the losses should be the frequency, which [10] indicates to occur at 300 kHz. On the other hand, the β values of the second and third sets of Steinmetz parameters are different. If one considers the 500 kHz frequency a hard limit between which set to use, continuity between core losses would be lost depending on the value of the flux density.

To avoid this issue, the core losses at any given point are calculated with the 3 set of Steinmetz parameters, and then the core losses are obtained as

$$P_c = \max \left\{ \begin{aligned} P_{c1} &= v_c k_1 \left(\frac{\sqrt{2} V_{RMS}}{2\pi A_c} \right)^{\beta_1} f^{\alpha_1-\beta_1} N^{-\beta_1} \\ P_{c2} &= v_c k_2 \left(\frac{\sqrt{2} V_{RMS}}{2\pi A_c} \right)^{\beta_2} f^{\alpha_2-\beta_2} N^{-\beta_2} \\ P_{c3} &= v_c k_3 \left(\frac{\sqrt{2} V_{RMS}}{2\pi A_c} \right)^{\beta_3} f^{\alpha_3-\beta_3} N^{-\beta_3} \end{aligned} \right\}. \tag{14}$$

This will remove discontinuities due to the change in β from the second and third Steinmetz parameter set. To better visualize this, the evolution of the losses for flux densities of 25, 50, 100 and 200 mT are shown in Fig. 5. As expected, there are no discontinuities at the 300 kHz limit, but this is not the case at the 500 kHz limit. If the proposed method with (14) is used the discontinuities at 500 kHz are removed. Regions for using one or another set of Steinmetz parameters can be defined as the points where $P_{c2} = P_{c3}$.

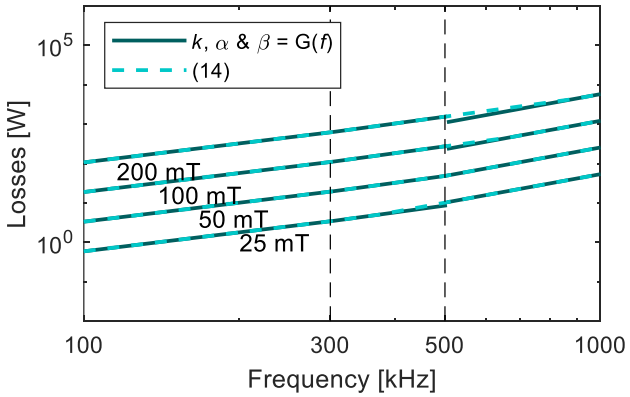

Fig. 5: Discontinuities in core losses if fixed frequency limits are higher loss case are assumed for the different Steinmetz parameter sets.

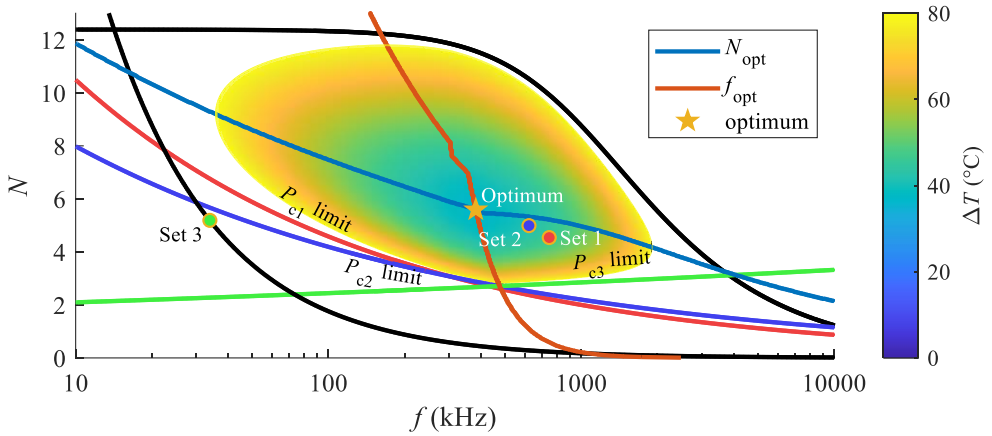

Fig. 6: Transformer design space taking the high frequency effects in the windings and core into consideration. Three core loss limits are shown, one for each set of Steinmetz parameters.

The optimal values for the number of turns and frequency also become discontinuous functions, thus first the set of Steinmetz parameters to use must be identified and then use (12) and (13) to estimate the optimal values. Note that in the case of the third set of parameters, the condition of $\alpha < \beta$ is not true, thus in (13) $f_{\text{opt}} < 0$ Hz. This is obviously not possible; thus, the optimal frequency will be where the boundary conditions $P_{c2} = P_{c3}$ meet.

The design space considering both high frequency effects in the windings and in the core is shown in Fig. 6. Note now that 3 optimum solutions are marked, which represent the optimal solutions estimated for each set of Steinmetz parameters. The optimal solution with the first set is equal to the one shown in Fig. 4 (747 kHz 4.54 turns). The optimal solution for the second set of parameters is similar to the first one, but due to an increased α parameter, it is found at a slightly lower frequency (621 kHz 4.99 turns). Lastly, the optimal solution for the third set of parameters is found at the flux density saturation limit (34 kHz 5.19 turns), since as previously discussed, (13) leads to $f_{\text{opt}} < 0$ Hz and the saturation flux density becomes the practical limit for the design frequency.

The true optimal solution in this case must be obtained by comparing the losses from the three regions and selecting the lowest loss design. In this case, the optimal solution appears between the boundaries of the second and third sets of parameters (383 kHz 5.59 turns).

V. Conclusions

This paper presents a holistic study of how high frequency effects regarding winding and core losses impact the design space of high frequency transformers.

First an overview of the classic design laws is presented, obtaining mathematical expressions for the different key design parameters for different number of turns and working frequencies. The obtained design space clearly depicts the benefits of increasing working frequency for transformer design, but without considering the high frequency effects the optimal design always appears at $f = \infty$.

Next, the effect of the increase in winding losses at high frequencies is added to the design space, which sets a high frequency limitation to the design space. Nevertheless, these calculations are carried out under the assumption that the Steinmetz parameters do not change, which is proven to not being true at high frequencies.

To check the effect of the variable Steinmetz parameters, the design space is analyzed for the different possible set of parameters. It is pointed out that the assumption that the parameters change discretely at given frequencies is only true as long as the β parameter does not change. To avoid discontinuities in the design space, the different sets are analyzed in the whole design space and the solutions combined accordingly.

The final design space demonstrates how not considering the variability of these parameters can lead to suboptimal solutions. Note that in most power applications, winding losses will be the main limitation in the transformer design, but the results obtained in this analysis can be of interest for planar and PCB based transformers where the copper losses are highly optimized.

References

[1] W. . -J. Gu et al, "A study of volume and weight vs. frequency for high-frequency transformers," *Proceedings of IEEE Power Electronics Specialist Conference*, 1993.

[2] M. Kasper et al, "GaN HEMTs Enabling Ultra-Compact and Highly Efficient 3kW 12V Server Power Supplies," *IEEE International Power Electronics and Application Conference and Exposition (PEAC)*, 2018.

[3] M. J. Kasper et al, "Ultra-high Power Density Server Supplies Employing GaN Power Semiconductors and PCB-Integrated Magnetics," *11th International Conference on Integrated Power Electronics Systems*, 2020.

[4] F. C. Lee, Q. Li, Z. Liu, Y. Yang, C. Fei and M. Mu, "Application of GaN devices for 1 kW server power supply with integrated

magnetics," in CPSS Transactions on Power Electronics and Applications, vol. 1, no. 1, pp. 3-12, Dec. 2016.

[5] G. Li and X. Wu, "High Power Density 48–12 V DCX With 3-D PCB Winding Transformer,"in IEEE Transactions on Power Electronics, vol. 35, no. 2, pp. 1189-1193, Feb. 2020.

[6] M. H. Ahmed, C. Fei, F. C. Lee and Q. Li, "48-V Voltage Regulator Module With PCB Winding Matrix Transformer for Future Data Centers," in IEEE Transactions on Industrial Electronics, vol. 64, no. 12, pp. 9302-9310, Dec. 2017.

[7] R. Yu, T. Chen, P. Liu and A. Q. Huang, "A 3-D Winding Structure for Planar Transformers and Its Applications to LLC Resonant Converters," in IEEE Journal of Emerging and Selected Topics in Power Electronics, vol. 9, no. 5, pp. 6232-6247, Oct. 2021.

[8] A. Arruti, J. Anzola, F. J. Pérez-Cebolla, I. Aizpuru and M. Mazuela, "The Composite Improved Generalized Steinmetz Equation (ciGSE): An Accurate Model Combining the Composite Waveform Hypothesis With Classical Approaches," in IEEE Transactions on Power Electronics, vol. 39, no. 1, pp. 1162-1173, Jan. 2024.

[9] M. Chen et al., "MagNet Challenge for Data-Driven Power Magnetics Modeling," in *IEEE Open Journal of Power Electronics*.

[10] S. A. Mulder, "Fit Formulae for Power Loss in Ferrites and their Use in Transformer Design," in proc. 26th International Power Conversion Conference (PCIM), 1993.

[11] Alex Van den Bossche, Vencislav Cekov Valchev, Inductors and Transformers for Power Electronics, Boca Raton, FL, Taylor & Francis Group, 2005.

[12] W. G. Hurley, W. H. Wolfle and J. G. Breslin, "Optimized transformer design: inclusive of high-frequency effects," in IEEE Transactions on Power Electronics, vol. 13, no. 4, pp. 651-659, July 1998

[13] M. Leibl, G. Ortiz and J. W. Kolar, "Design and Experimental Analysis of a Medium-Frequency Transformer for Solid-State Transformer Applications," in IEEE Journal of Emerging and Selected Topics in Power Electronics, vol. 5, no. 1, pp. 110-123, March 2017.

[14] W. G. Hurley, E. Gath and J. G. Breslin, "Optimizing the AC resistance of multilayer transformer windings with arbitrary current waveforms," in IEEE Transactions on Power Electronics, vol. 15, no. 2, pp. 369-376, March 2000.

[15] T. Guillod and J. W. Kolar, "Medium-frequency transformer scaling laws: Derivation, verification, and critical analysis," in CPSS Transactions on Power Electronics and Applications, vol. 5, no. 1, pp. 18-33, March 2020